energies

MDPI

Article

Selected Simulation and Experimental Studies of the Heat Transfer Process in the Railway Disc Brake in High-Speed Trains

Jacek Kukulski [1,*], Andrzej Wolff [1] and Sławomir Walczak [2]

[1] Faculty of Transport, Warsaw University of Technology, 00-662 Warsaw, Poland; andrzej.wolff@pw.edu.pl
[2] Railway Research Institute, 04-275 Warsaw, Poland; swalczak@ikolej.pl
* Correspondence: jacek.kukulski@pw.edu.pl

Abstract: The effectiveness of railway brakes strongly depends on their thermal condition. A computer simulation and experimental investigations on a full-scale dynamometric stand were chosen as an adequate analysis of the heat transfer process in brakes. The article introduces a two-dimensional, axisymmetric numerical model of the tested disc brake. Boundary conditions related to the heat generated in the friction brake and heat transferred to the environment are also presented. The transient heat transfer problem was solved using the in-house computer program of the finite element method. The article presents simulations and experimental investigations of the intensive braking of a train with an initial high speed. Temperature responses of the disc brake on the friction surface and at other selected points are shown. In addition, a thermal imaging camera was used to assess the temperature distribution on the friction surface of the disc. The results of experimental and simulation tests were preliminarily compared. Similar maximum temperature values were obtained at the end of braking with a particular discrepancy in temperature responses during the analyzed process.

Keywords: dynamometric stand; heat transfer in brakes; simulation tests

Citation: Kukulski, J.; Wolff, A.; Walczak, S. Selected Simulation and Experimental Studies of the Heat Transfer Process in the Railway Disc Brake in High-Speed Trains. *Energies* **2023**, *16*, 4514. https://doi.org/10.3390/en16114514

Academic Editors: Grzegorz Karoń, Muhammad Sultan, Robert Tomanek and Dariusz Pyza

Received: 1 April 2023
Revised: 26 May 2023
Accepted: 30 May 2023
Published: 4 June 2023

1. Introduction

Braking systems are among the main factors that affect railway vehicles' operational reliability and safety. They are used in all types of trains. The operation of brake systems in conditions of increased functional requirements, related to the increase in operating speed, load and frequency of operation, makes it necessary to consider the effects of the dynamics of the structure in the design. In addition, the increase in operation speed, vehicle weight and use of new materials for the elements of friction pairs cause further problems in brake systems.

Thermal processes accompany the work of railway and car brakes. They are of great practical importance because they significantly affect the functioning of brakes and the intensity of wear of friction elements and may cause damage to these elements. The temperature fundamentally influences the course of tribological phenomena on friction surfaces. Along with its increase, the friction coefficient changes—as a rule, it decreases, which reduces the braking effectiveness [1–6].

The resistance of the friction pair to abrasive wear is also reduced. In extreme cases, structural and chemical degradation of the friction material may occur [1–6]. The increase in temperature, in combination with the phenomenon of thermal expansion, causes deformations and thermal stresses, which cause temporary disturbances in the cooperation of friction pairs. A known effect of cyclical stresses is cracking the drum or disc material starting at the friction surface and advancing into the material [1,7].

For all these reasons, the thermal phenomena of brakes are the subject of numerous experimental and theoretical studies [1–3,7–20].

Improving the tribological performance of railway brakes has become an important subject. A thorough analysis of the following topics is needed:

- A proper operation of the braking system, including the friction pairs of the rail brake, requires a systematic diagnosis of its condition, as high local temperatures may lead to unacceptable deterioration of braking effectiveness, such as braking failure.
- Generated frictional heat during the braking causes several adverse effects on the brake system, such as premature wear, thermal cracks and variations in the thickness of railway brakes, so it is essential to precisely define the temperature fields and thermal stresses of such friction pairs (brake pad, disc brake).
- There are no data in the literature on effective analytical methods of heat transfer in railway brakes up to high speed, which would enable the determination of the temperature distribution.
- The proposed research method of the heat transfer process in railway brakes allows the assessment of the temperature distribution on the friction surface of the brake disc during the high-speed braking.
- In addition to the proposed research method, experimental tests were carried out on a full-size dynamometric test bench using various tools for measuring temperature, enabling the evaluation of the method used.

2. Review of the Literature

2.1. Thermal Phenomena in Brakes

As a result of friction occurring in brake discs, mechanical energy is converted into thermal energy. Research on thermal phenomena in rail and car brakes has been carried out and continues in many research centers in Poland and abroad. The article divides the literature review into several areas concerning the study of brake friction pairs. In both experimental tests and computer simulations, the phenomena of the formation of hot regions on the friction surface of disc brakes and the phenomenon of residual stresses appearing during the significant thermal loads of the friction pair were taken into account.

The article [21] presents an experimental method of testing the convective heat transfer concerning ventilation ducts applied in disc brakes. In order to simulate the operating conditions of the ventilation ducts, the naphthalene sublimation method was used to obtain the tested heat convection. The correlation between the Coriolis acceleration and the heat transfer coefficient is an interesting observation from simulation studies.

In Reference [22], a simulation model of the railway disc brake was created, which was used to check the significance of various assumptions. Using the model, the authors researched the impact of friction material properties on the disc brake temperature response. The developed heat transfer model can be used for calculations according to EN 14535-3 [23], preceding the experimental tests of new disc brakes for compliance with this standard.

The study [24] involved analyzing and characterizing the transfer, by conduction between the disc and the brake pads, for the automotive system. This work made it possible to perform comparative tests of the temperature course in the disc brake during braking. Authors were concerned with the differences between the analytical and numerical solutions of the heat transfer equation in the brake disc and linings in real conditions. Another interesting study [25] concerns the convective heat transfer characteristics of the track surface on which wheels roll over periodically. In this work, an experimental model was used to determine the coefficient of convective heat transfer on the track's rolling surface from the rail vehicle's wheels. The results show that the heat transfer coefficient concerning the vehicle speed depends on the diameter of the wheel.

2.2. Experimental and Simulation-Based Tribological Research

Experimental tests of this type can be carried out on dynamometric test stands, often on a 1:1 scale. Such test rigs are very complicated and complex objects and, at the same time, are costly to build and maintain. Therefore, few research centers or producers of friction pairs of brakes can afford such a dynamometric test stand. During complex tribological

and thermal processes, the experimental tests require appropriate measuring equipment to ensure the excellent quality of measurements. To maintain the required quality and repeatability of results, this type of laboratory is often accredited or certified by national or international accreditation bodies. Tests carried out on such accredited stands are performed under European Standards (EN), UIC Leaflets, or specifications of brake friction pair manufacturers. The trials of frictional properties are used to determine the average coefficient of friction of the friction pair. These tests are often performed for dry and wet conditions simulating rain or snowfall. Such tests are designed to detect mixed friction or aquaplaning, which can significantly extend the braking distance. Tests of resistance to thermal loads are undertaken to check how the friction pair would behave under extreme thermal loads. These loads may appear in several cases, including:

- When braking from high speeds, 350–400 km/h;
- Failure of the friction brake (blocked friction pair);
- Going down a steep slope of the railway line (21–40‰).

These types of experimental tests are characterized by significant braking energy and power. Moreover, tested objects subjected to substantial thermal loads are subject to extreme wear and permanent damage. Numerous works on the tribology of friction pairs have been presented, including the study [26]. The authors of [10] showed the results of tests obtained on actual objects of the rail vehicle braking system, showing the phenomenon of generating hot areas during the tribological tests of friction pairs of rail brakes. Such phenomena reduce the braking effectiveness and cause chemical changes in the structure of brake elements made of organic materials. Reference [11] investigates the heat transfer caused by friction in brake systems used in high-speed rail vehicles. In [27], the author described bench tests of sintered brake pads at an initial speed of 300 km/h and presented the tribological results of these tests.

In their work [28], the authors presented experimental and simulation tests of brake shoes for motor vehicles. In addition to basic tribological tests, vibration and noise measurements were performed in dry and wet conditions. The experimental tests were performed on a non-standard small-scale dynamometer. Friction materials of various geometric shapes were tested. The influence of brake lining shapes on the formation and characteristics of vibrations and noise were assessed and analyzed. The results revealed that different geometries of brake linings show differences in dry and wet conditions. All the tested samples generated vibrations in dry conditions. A triangular lining caused the most considerable vibrations and the highest sound pressure level. The reason is high contact stress on the front edge of the triangular lining. Under wet conditions, no vibration noise occurs for the circular-shaped insert. Only intermittent oscillations of the vibration signals are observed for the triangular and hexagonal blocks.

On the other hand, in [14], simulation tests were carried out to assess the impact of various materials commonly used to produce disc brake components. Special requirements have been taken into account, such as high-load operation, including those used in racing cars. The applied finite element (FE) models, in addition to a detailed FE model of the entire disc brake, also included the wheel hub and the steering knuckle, elements which were verified using an experimental modal analysis. The Taguchi method [14] allowed the assessment of various materials' contributions and their interaction's effects to reduce noise in squeaks effectively. The results showed that the brake shoe/friction material contribution to the total system instability (squeal generation) is 56%. The rotor material contributes 22% to system instability. The materials of clamps and locks account for 11%.

In the paper [29], the research related to the behavior of materials used for brake discs, such as cast iron, chrome steel and metal matrix composites, was carried out under the influence of thermal fatigue. First, the samples used in the tests were heated to a specific temperature and then quickly cooled. Then, wear tests were carried out using a pin-on-disc tribometer. The test results showed that the thermal load influences the structure of the contact surfaces of all tested samples by increasing their roughness. In addition, the wear

rate of friction materials has increased, and, interestingly, thermal fatigue has no significant effect on the friction coefficient.

In [30,31], a new approach to numerical simulation using the finite element method was proposed. Models of full disc brakes and discs with ventilation channels were developed. Relevant, three-dimensional models of heat transfer in friction pairs were built. The simulation results justified the possibility of simplifying the shape of the disc's ventilation channels. The share of energy dissipated due to convection and thermal radiation to the environment was also analyzed. It confirmed compliance with the results of experimental studies while maintaining the same braking parameters. In another study by the same authors [32], a simulation model was created to determine the transient temperature field in the ventilated disc brakes of the traction diesel multiple units (DMUs). Simulation tests were carried out with a division into the brake lining and rotor. The obtained results of temperature distribution were compared with experimental tests using thermocouples.

A more accurate and efficient method of predicting the temperature field in brakes was presented in the paper [33]. The method of an evenly distributed heat source using the cosine function was applied here. The predicted maximum temperature errors could be reduced to 7%. The following work [34] presented an unsteady heat transfer model in ventilated disc brakes. Relevant heat energy changes during the braking process were shown. It was concluded that the heat generated in the disc brake increases non-linearly while dissipating linearly. The heat of a ventilated disc brake increases with the duration of braking, but its rate of increase steadily decreases.

2.3. Hot Spot Problems

Hot spotting appears where we deal with friction, e.g., in clutches, brakes of cars and railways and other sliding systems [5]. In the case of sliding motion, heat is generated by friction at the interface of two elements in relative motion. It is recommended that the distribution of the heat generated by friction is even over the entire surface of the object, resulting in an even thermal load. However, the geometrical imperfections of the cooperating surfaces (friction pairs) and the appearing deformations cause the heat distribution to differ on the surface of the elements [6]. In the case of clutch plates, hot spots can be caused by design features that cause uneven pressure distribution on the sliding surfaces. Such causes of hot spots are easy to locate and thus eliminate. It should be noted, however, that most of the observed hot spots are not related to the geometry of the interacting surfaces. Appearing hot spots often do not correlate with subsequent hot spot patterns. Their formation mechanism is the interaction between thermal deformations and heat distribution.

The formation mechanism of hot spots and areas was well identified and described by James R. Barber, who studied hot spots in railway brakes [35]. According to the author, the local heat generation due to friction is proportional to the local contact pressure of the elements. In areas with higher contact pressure, a higher temperature rise is registered. The increased local thermal expansion further increases along with the concentration of pressure. It creates a positive feedback loop causing system instability, referred to as Barber thermoelastic instability (TEI), which is friction-induced. Currently, this abbreviation is often used in scientific publications.

As a result of friction occurring in disc brakes, mechanical energy is converted into thermal energy. In the case of brake systems used in motor vehicles (road and rail), this phenomenon arises due to the frictional interaction of the brake pad with the disc surface [1,4,11,35–38]. The heat accumulated in the friction elements of such systems causes thermal disturbances, which result in the emergence of disadvantageous phenomena. One of them is the development of hot areas on their surfaces [2]. The formation of hot spots is caused by high thermal gradients, locally inducing high stresses in the surface structure of the friction pairs. High local temperatures can lead to an unacceptable reduction in braking performance, such as loss of braking or undesirable low-frequency vibrations [9,39,40]. Heat is generated in its friction elements during the braking at high speeds and intense

pressure in the brake system. One of the negative phenomena affects the softening and melting of materials on the contact surfaces of friction elements.

Furthermore, it generates an increase in thermal deformation and unit pressure. As a result, clean metal surfaces may be exposed and brought closer to the distance of intermolecular forces. The consequence is tacking and damaging the friction surfaces by removing particles from them and smearing them on their surface in a further braking step. As a result, the contact area is limited to local places that are commonly referred to as hot spots. Depending on their form, they can be classified as apex, focal, deformation, band, zonal and mixed regions [39].

Another classification of hot areas in brake systems was carried out by French researchers [41], who were the first to propose a five-class division of hot spots for the railway brake disc. It was performed based on the obtained results of experimental research. This division was created from the thermal maps describing the temperature distribution on the brake disc (Figure 1). Those classes are defined as spot hot spots, fringe hot spots, hot bands, macroscopic and regional hot spots.

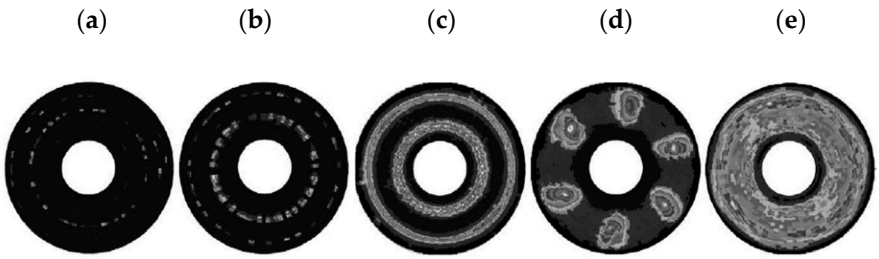

Figure 1. Classification of hot spots: measurements with an infrared camera [42] (**a**) rough group; (**b**) fringed hot spots; (**c**) hot strands; (**d**) macroscopic hot spots; (**e**) regional hot spots.

The first type of division shown in Figure 1a, defined as rough, is characterized by a rapidly increasing temperature over a short period of time on very small areas of the contact surface of the friction pair element. The main parameters influencing this phenomenon are the rheological properties of the contact surface and its topography. The second type of classification was defined as a gradient (Figure 1b). It corresponds to small areas of contact appearing along the single contact path of the friction pair. It is due to contact instability and thermoelastic instability of the block structure. In turn, the hot bands shown in Figure 1c are formed in the frictional contact areas of the disc, where the pressure of the frictional pair is reduced. They appear as narrow, high-temperature rings aligned with the rotation of the dial. During braking, they move in the radial direction, depending on changes in the pressure surface in the contact area. The next group is a macroscopic group represented by thermal areas regularly distributed on the plate surface (Figure 1d). Their appearance on the disc brake resembles the buckling of its surface. This phenomenon intensively reduces the contact surface via the wavy deformation of the disc under the influence of high thermal load. The last group consists of regional hot spots (Figure 1e). The reason for such a phenomenon is the non-uniform cooling of the disc, and such areas appear at the end of braking as a result of thermal diffusion and non-uniform cooling resulting, among others, from the design of the brake disc.

One of the negative phenomena accompanying the above-mentioned hot spots and areas is the thermal overheating of the materials of the friction elements where they occur. The formation of such regions is considered one of the main mechanisms of disc brake degradation and destabilizing the braking process [43]. Such high local temperature rises may also lead to an unacceptable reduction in the braking performance, such as a reduction in the brakes' effectiveness due to a lower coefficient of friction or a smaller contact surface of the friction elements due to undesirable vibrations and deformation of these elements.

Hot spot areas on the friction surface of the brake disc are a more recognized problem in road transport, but such phenomena are often visible in railway research. The appearance

of hot areas on the friction surface of the brake disc is shown in Figures 2 and 3 (visual images and photos from a thermal imaging camera).

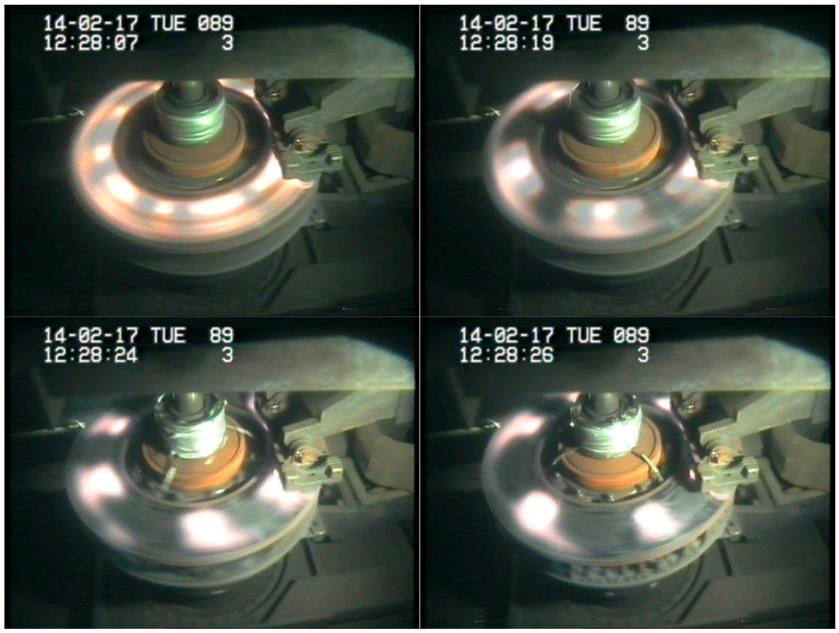

Figure 2. View of the different classes of hot areas on an axle-mounted brake disc in the final stage of braking from high speeds of 385 km/h.

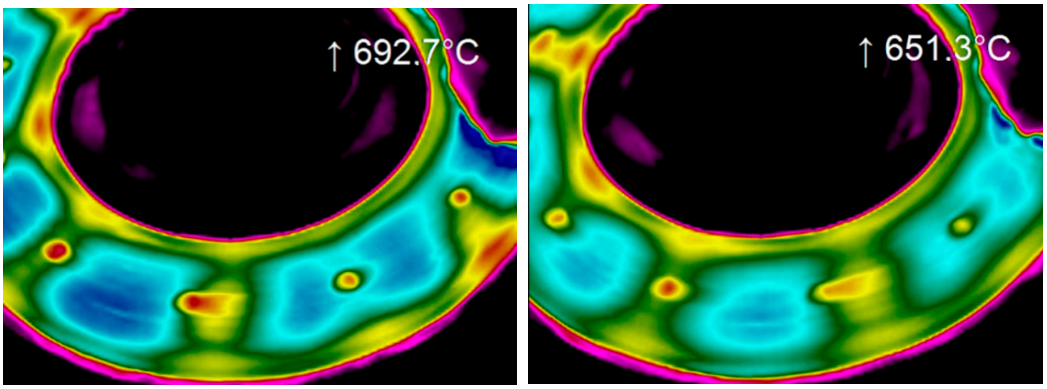

Figure 3. Temperature distribution on the wheel-mounted disc brake in the final stage of braking from a speed of 385 km/h.

The images from the video camera (Figure 2) show the stages of the formation of hot areas on the ventilated brake disc. The tests were carried out for organic material and a cast steel disc with 640/110 mm dimensions. The initial speed of the test was 385 km/h. Extreme test conditions, both in terms of load (simulated braked mass, downforce) and speed, made it possible to capture such a phenomenon without using a thermal imaging camera. After the tests were completed and the brake disc cooled down, discolorations in the form of black dots were visible on the disc, indicating local hardening of the material.

A similar test to that of the disc mounted on the axle was performed for the disc brake mounted on the wheel. Such solutions are used more often in electric multiple units (EMUs), where there is usually not enough space on the axle to mount the disc brake there because the traction motor often occupies this place. It applies only to drive bogies, as axle discs can be installed on rolling bogies. The thermographic images presented in Figure 3, this time obtained using a thermal imaging camera, show the formation of the hot areas between the bolts securing the friction ring to the wheel surface. The images show that

high temperatures at such high friction braking speeds contribute to the emergence of phenomena such as hot spots.

2.4. Residual Stresses

Residual stresses often appear due to significant thermal loads occurring during the braking, e.g., from high speeds or damage to the friction brake (the so-called brake lock). Measurements of residual stresses in brake discs are complicated to implement due to their design, among other factors. There are more possibilities when testing railway wheels. This area is more recognized and much more critical from a security point of view. Damage to wheels related to thermal effects during braking, starting from thermal cracks in the rim, has been a severe rolling stock problem. Overheating the wheel causes the surface color to change. The more intense the overheating, the greater the range of the color change zone. Thus, the cracking caused by thermal shock results from unfavorable changes in residual stresses in the wheel rim. These stresses in new monoblock wheels are usually compressive. During the heating and cooling of the wheels, the compressive stresses change into tensile stresses due to the use of brake pads. However, attempts are made to assess the residual stresses in a disc brake, either with the help of computer simulations or with the measurement of neutron diffraction regarding the levels and distribution of stresses in the applied cast iron rotor of the disc brake [15]. Tests and analyses of thermal stresses in a ventilated brake disc were also carried out using the three-dimensional models for two cases (regardless of whether the pressure distribution on the contact surface is uniform). First, the pressure distribution analysis was carried out to determine the pressure distribution on the contact surface. In places where the maximum thermal stresses occur in variable pressure distribution, they are similar to the area where fatigue cracks arise in an actual brake disc [38,44,45].

2.5. Literature Review Summary

The presented review of the literature in the field of heat transfer research in railway brakes can be summarized as follows:

- In papers [26,38], only experimental tests on a dynamometric stand were carried out, within which friction coefficients were determined together with their evaluation. In addition, temperature distributions were obtained using thermocouples. Initial braking speeds did not exceed 300 km/h;
- In publications [27,31], only simulation studies using commercial applications of the finite element method (FEM) were carried out. The tests included the distribution of thermal stresses and temperatures or the friction study of the brake linings against the disc for single braking from a maximum speed of 100 km/h;
- Simulation and experimental studies:
    - Heat transfer simulation studies using commercial applications of FEM and also experimental studies, including tests (of a brake disc mounted on a wheel) in the range of temperatures that occur during braking [11];
    - Simulation tests covering the course of temperatures during braking at selected points of the brake rotor. Numerical brake disc models with ventilation channels and friction linings were built. Commercial FEM applications were used. Experimental studies also covered temperature courses during braking from speeds up to 100 km/h [30];
    - Simulation studies using commercial FEM applications involving stress distribution. A mathematical model of heat transfer in brakes was built. Experimental tests were also carried out, including temperature measurements with thermocouples on (a disc brake mounted on a wheel). Initial braking speeds reached 160 km/h [32];
    - Computer simulations were performed. A new method of predicting the maximum disc temperature was described. It was followed by experimental

verification. Investigations with initial braking speeds of v = 40–100 km/h were realized [33];
- Simulation tests concerning temperature and stress distributions of the ventilated disc brake were performed. In addition, experimental tests with appropriate temperature measurements were carried out. Initial braking speeds reached v = 250 km/h [34];
- FEM simulation and experimental tests on a stand with reduced (compared to reality) dimensions [45].

2.6. Present Study

In this paper, relevant experimental and computational results for railway brakes are presented.

An in-house, specialized computer program of the finite element method was developed. Much earlier, the convergence of its algorithm was verified. Its rapid use and support for test bench research were ensured. The computational heat transfer model was newly applied for rail transport purposes. Previously, it was often used to assess the thermal states of automotive brakes.

Required numerical methods are very specific, and heat transfer problems cannot be solved by all-purpose commercial software like in papers [11,27,30–32,45]. The development of specified numerical codes dedicated for application in the railway transport industry is one of the key problems. Such codes have been developed only by a few scientific groups and are not widely available. Due to that fact, developing the in-house specialized program seems to be a significant achievement.

Experimental tests were carried out on a full-scale dynamometer stand. It has, as one of the seven stands in the world, International Union of Railways (UIC) homologation for testing the friction pairs of the railway brake. Numerous tests performed for manufacturers of friction pairs in Europe and around the world made it possible to adapt this stand to the latest customer requirements. It should be emphasized that the presented studies were carried out at high initial braking speeds V_{max} = 350 km/h—higher than in papers [26,27,30–34,38].

Another significant aspect of this paper is the "hot spots" phenomenon described in Section 2.3. Recorded images of the formation of "hot spots" using an infrared camera are presented. This phenomenon only occurs under certain extreme conditions. It is mainly recorded at high thermal loads when the sliding speed of the brake lining exceeds 50 m/s. During the tests, sliding speeds of 54 m/s at the initial braking speed of 350 km/h were obtained.

Although the "hot spots" phenomenon was not computed, the results of our observations are presented. These situations are unacceptable from the point of view of regular brake operation.

The presented experimental and computational studies, including the methods used, may help optimize the friction pair exposed to high thermal loads. Excessive thermal state may result in faster wear of the lining material. Therefore, pollution of the natural environment is observed in the vicinity of the railway track in the form of intensive dusting.

3. Heat Transfer Model in Railway Brakes

3.1. Mathematical Model of Heat Conduction

The heat transfer in the brake should be considered as a transient process. The reason is that the following are variable in time: heat generated during the braking and dissipated to the environment and the temperature field of brake frictional elements.

The primary task is to choose a suitable mathematical model of the heat transfer in railway brakes (Figure 4). In practice, heat conduction plays a significant role through the brake rotor (here: disc).

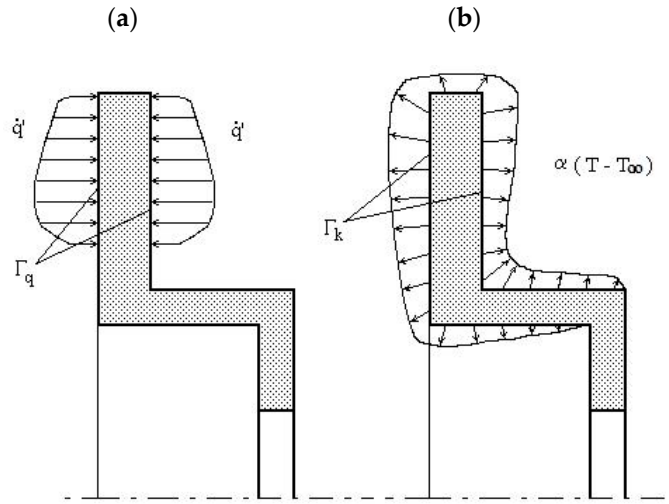

Figure 4. General physical model of the heat transfer in a disc brake: (**a**) heat generated on the frictional surface Γ_q of the brake, (**b**) heat transferred to the environment from rotating surfaces Γ_k.

Analyzing the geometric shapes of solid disc brakes (i.e., without internal vents), we can assume they are axisymmetric. However, such symmetry does not apply to boundary conditions of the heat transfer problem under consideration. It is necessary to note that friction pads under which the heat flux is generated cover only a part of the disc perimeter (brake rotor). Apart from this, the pressure distribution on the disc's perimeter is uneven, so the heat flux is not uniformly distributed. We need to remember, however, that the rotor rotates relative to linings. For this reason, the assumption of axisymmetry of the heat flux on frictional surfaces means only time-averaged boundary conditions in the period corresponding to one rotation of the disc brake. This kind of simplification ends up with a minor mistake, particularly at the high rotational speeds of the brake rotor.

For the reasons above, a two-dimensional, axisymmetric model was chosen to simulate the heat transfer phenomena in railway brakes.

In this case, the heat conduction equation will take the following form [46]:

$$\rho c_p \frac{\partial T}{\partial t} = \frac{1}{r}\left[\frac{\partial}{\partial r}\left(r\lambda\frac{\partial T}{\partial r}\right) + \frac{\partial}{\partial z}\left(r\lambda\frac{\partial T}{\partial z}\right)\right] \tag{1}$$

where:

c, λ, ρ—mass density, specific heat and thermal conductivity of the rotor;
r, z—cylindrical coordinates;
T—temperature;
t—time.

The heat flux q' is generated on friction surfaces of the rotor Γ_q (Figure 4a). Here are boundary conditions of the II type in the form [16–19,46]:

$$-\lambda\frac{\partial T}{\partial n} = \dot{q}'(r,z,t) \tag{2}$$

wherein:

$$\dot{q}' = \xi\dot{q} \quad \text{and} \quad \dot{q} = \mu p v \tag{3}$$

where:

ξ—a ratio of heat flux partition between the rotor and friction linings;
μ—friction coefficient;
p—contact pressure at the interface rotor—brake lining;
v—slip velocity.

The heat transfer to the environment occurs on the free surfaces Γ_k (Figure 4b). It is described by boundary conditions of the III type in the form [16–19,46]:

$$-\lambda \frac{\partial T}{\partial n} = \alpha [T(r,z,t) - T_\infty] \tag{4}$$

wherein:

$$\alpha = \alpha_k + \alpha_r \tag{5}$$

where:

α_k—convection-based heat transfer coefficient;
α_r—radiation-based heat transfer coefficient;
T_∞—ambient temperature.

The initial condition for the problem under consideration is as follows [16–19,46]:

$$T(r,z,t_0) = T_0 \tag{6}$$

where:

T_0—initial temperature.

3.2. Boundary Conditions of the Problem

Boundary conditions are integral parts of every mathematical model. First, heat flux distributed between a disc (brake rotor) and friction linings is generated on frictional surfaces. The most significant part of this flux is transferred to the rotor due to the considerable difference between:

- Values of thermal parameters of friction pair materials;
- Areas of the active frictional surface of both pair elements [16,17,19].

The heat flux generated in the brake examined on the inertia test bench was established as specified in Section 5.2 of this article (Equation (7)).

Secondly, there is a complex heat transfer with the environment on the free surfaces of the brake, based primarily on convection and, to a lesser extent, on radiation. The impact of radiation rises substantially only at very high temperatures (300–500 °C). A challenging task is to establish the value of the coefficient of the convection-based heat transfer with the environment. The complexity of the brake outflow by the cooling air and the variability of these conditions should be noticed. As a rule, the above-stated parameter is determined using criterion formulas of similarity theory [16–19,46]. Our computer software for generating boundary conditions of the II and III types, called GENTGV, has been developed (Equations (2)–(5)).

Interestingly, the flow around brakes and convection-based heat transfer in the last couple of years has been modeled using the computational fluid dynamics (CFD) method [3,13,42].

3.3. The Numerical Method Used to Solve the Problem

First, the possibility of solving the brake thermal conductivity using three numerical methods was studied: the finite difference, finite element and boundary element [4]. As a result of the analysis above, the finite element method was chosen. It was primarily due to the following factors: the all-purpose nature of its algorithm and widespread presence and the capability of precise approximation of the edge of the analyzed objects. Elements of axisymmetric shape were used. In their axial sections, these are four-sided, eight-node elements with straight or curved edges (second-order isoparametric elements) [4]. For analysis of the heat transfer in brakes, the relevant computer program of the finite element method called FEMHEAT was developed [16,17,19].

4. Experimental Testing

4.1. Dynamometric Bench

The experimental tests were conducted on the specialized inertial braking bench intended to test friction pairs of brakes of rail vehicles at the Railway Research Institute in Warsaw. The International Union of Railways (UIC) has certified the test bench for all-purpose test benches with a maximum speed of 420 km/h. The test bench design allows testing friction pairs of pneumatically activated railway brakes dedicated to high-speed fixed-formation trains, train units, locomotives and railbuses of actual size. In Figure 5, the stationary test stand, as well as mechanical flywheels, are shown.

(**a**) (**b**)

Figure 5. Test stand: (**a**) general view, (**b**) mechanical flywheels.

The primary technical parameters of the inertial test stand are presented in Table 1.

Table 1. Basic technical parameters of the inertial test stand.

Item	Parameter	Value
1.	Range of vehicle speed (for wheel ∅ 890 mm)	3.5 ÷ 420 km/h
2.	Maximum rotational speed	2500 rpm
3.	Driving motor power at 1150 rpm	536 kW
4.	Torque up to 1150 rpm	4450 Nm
5.	Max. braking torque: -Braking to a halt -Continuous braking	 3000 Nm 4450 Nm
6.	Range of moments of mass inertia with electric simulation	150 ÷ 3000 kgm^2
7.	Maximum simulated mass per friction pair	15,000 kg
8.	Range of total pressure force adjustment for brake shoes of the disc brake	0 ÷ 60 kN
9.	Range of temperatures for the disc brake (road wheel)	273–1273.150 K (0 ÷ 1000) °C

4.2. Test Scenarios

Bench tests of a cast steel solid disc without internal vents (dimensions: 640/45 mm) were carried out. Sintered disc brake pads with a total contact surface of 40,000 mm^2 (400 cm^2) were adopted. These brakes were used in the first TGV trains manufactured by Alstom. Table 2 depicts selected research programs for the solid disc brake (without internal vents) mounted on the axis.

Table 2. Test scenarios for solid disc brake mounted on the inertial stand shaft.

	Parameters of the Test Stand during Testing			
	v_0 (km/h)	F (kN) (Apply Force on Brake Linings)	m (kg) (Braking Mass)	T_a (°C) (Temperature at the Outset of Braking)
Test no. 2	200	18	5000	82
Test no. 3	250	18	5000	82
Test no. 4	300	18	5000	88
Test no. 10	350	14/18	5000	70

The temperature of the disc brake was measured on its friction surface using special slip thermocouples (Figure 6) and an infrared camera.

Figure 6. Research object, slip thermocouples and infrared camera.

4.3. Test Results

The results of experimental tests of two braking cases are demonstrated in Table 3 and Figures 7–14.

Table 3. Results of experimental tests of three cases of braking.

Test No.	v_0 (km/h)	Braking Energy (MJ)	Braking Power (kW)	Braking Distance (m)	Average Friction Coefficient	Average Temperature of Friction Surface at the End of Braking (Slip Thermo-Couples) T_{max} (°C)	Average Temperature of Friction Surface at the End of Braking (Infrared Camera) T_{max} (°C)
2	200	7.26	171	2347.7	0.343	212	208
3	250	11.36	208	3661.8	0.336	298	264
4	300	16.83	245	5551.3	0.323	383	378
10	350	22.77	218	8926.5	0.312	470	480

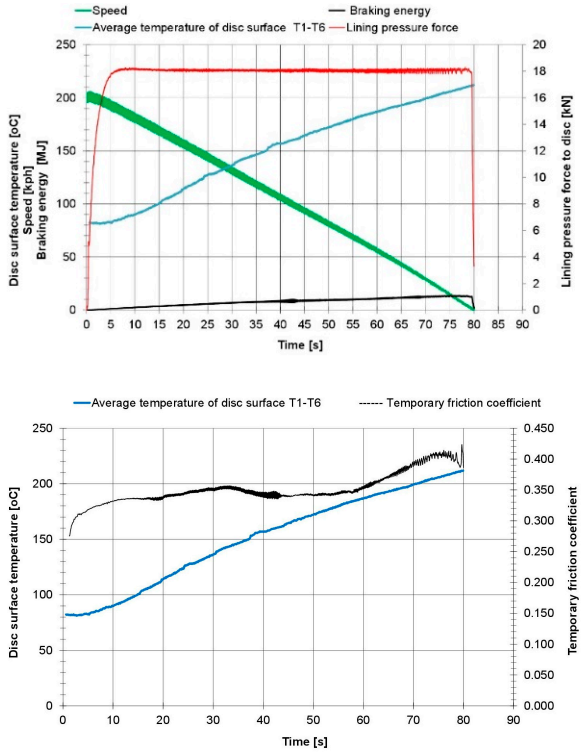

Figure 7. Pressure force of linings, friction coefficient, the average temperature of the disc surface and braking energy versus time for braking from the initial speed v_0 = 200 km/h (test no. 2).

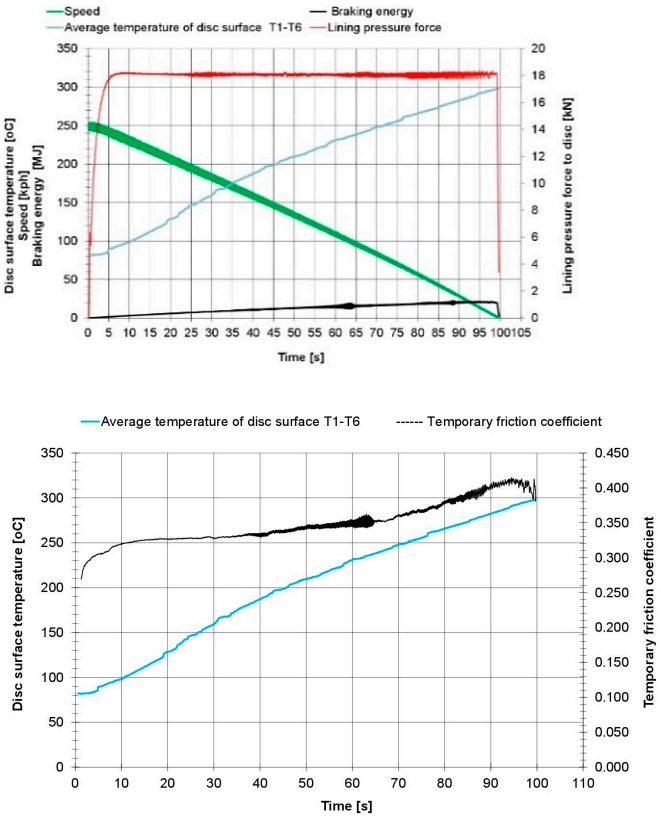

Figure 8. Pressure force of linings, friction coefficient, the average temperature of the disc surface and braking energy versus time for braking from the initial speed v_0 = 250 km/h (test no. 3).

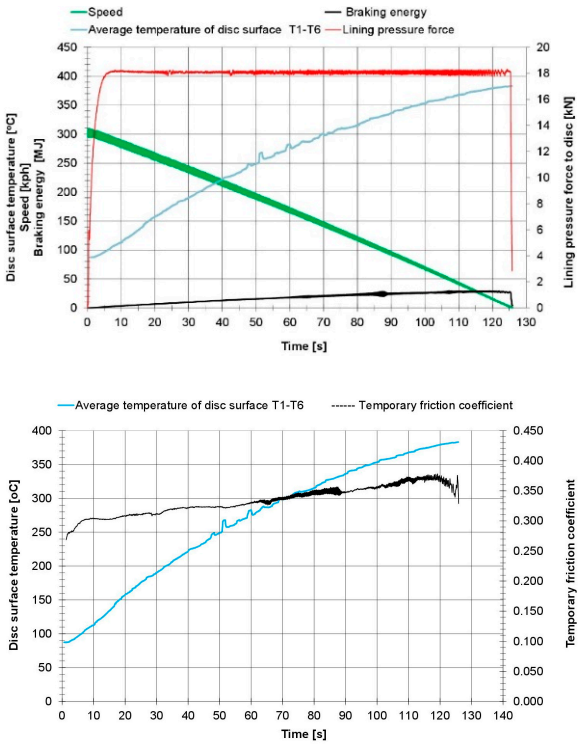

Figure 9. Pressure force of linings, the average temperature of the disc surface and braking energy versus time for braking from the initial speed v_0 = 300 km/h (test no. 4).

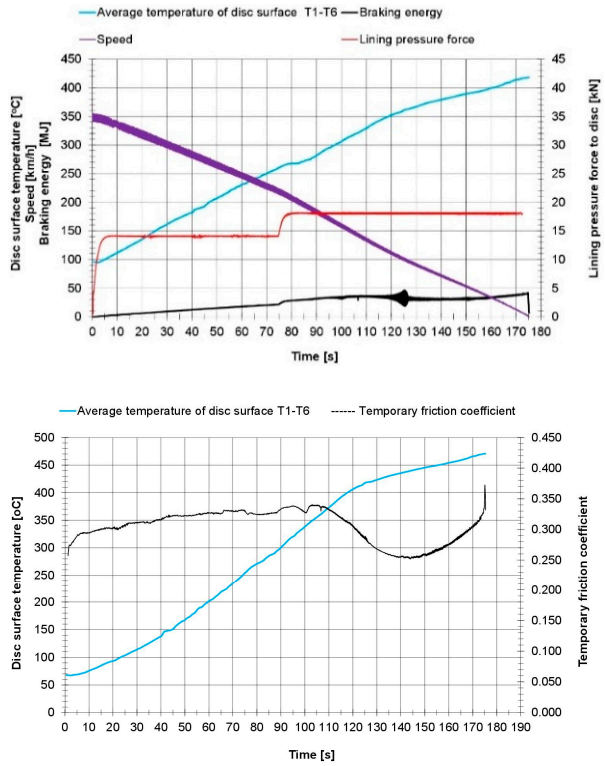

Figure 10. Pressure force of linings, friction coefficient, the average temperature of the disc surface and braking energy versus time for braking from the initial speed v_0 = 350 km/h (test no. 10).

(**a**) (**b**)

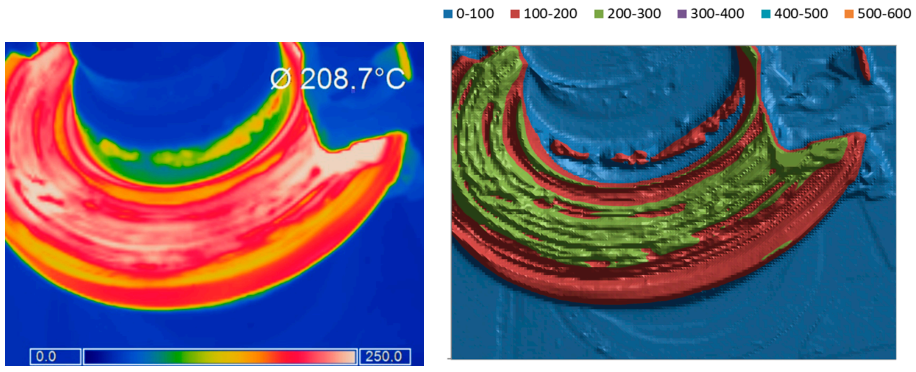

Figure 11. Temperature distribution on the disc brake (and its hub) at the end of braking from the initial speed of 200 km/h (test no. 2), (**a**) photos from the software of the thermal imaging camera, (**b**) exporting numerical data to MS Excel.

(**a**) (**b**)

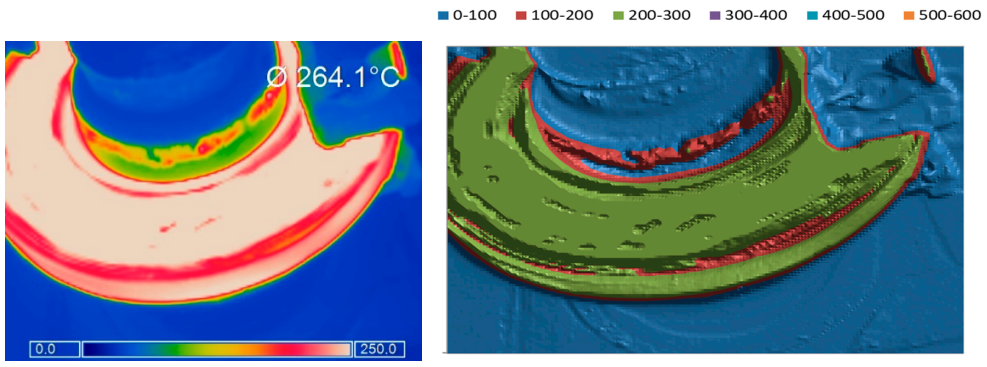

Figure 12. Temperature distribution on the disc brake (and its hub) at the end of braking from the initial speed of 250 km/h (test no. 3), (**a**) photos from the software of the thermal imaging camera, (**b**) exporting numerical data to MS Excel.

(**a**) (**b**)

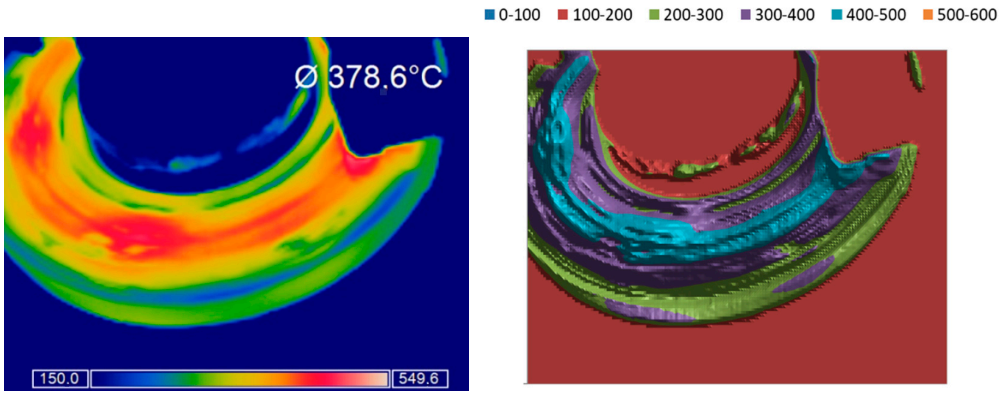

Figure 13. Temperature distribution on the disc brake (and its hub) at the end of braking from the initial speed of 300 km/h (test no. 4), (**a**) photos from the software of the thermal imaging camera, (**b**) exporting numerical data to MS Excel.

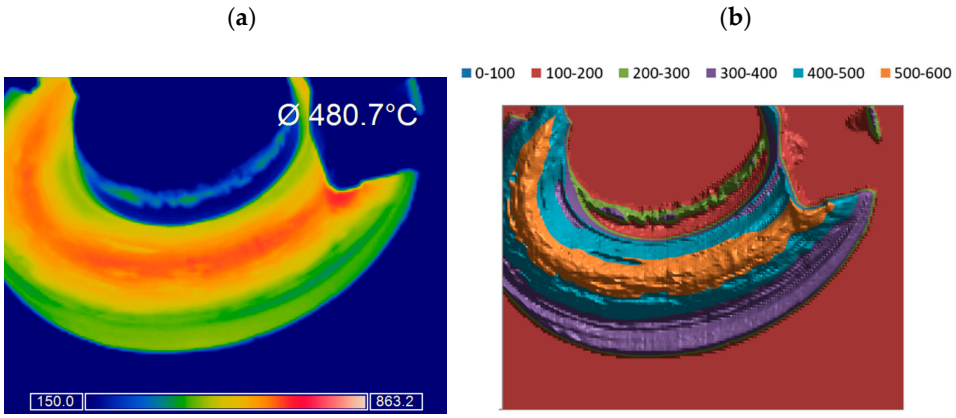

Figure 14. Temperature distribution on the disc brake (and its hub) at the end of braking from the initial speed of 350 km/h (test no. 10), (**a**) photos from the software of the thermal imaging camera, (**b**) exporting numerical data to MS Excel.

Figures 7–10 illustrate recorded parameters, such as average temperatures of the friction surface from six slip thermocouples, railway vehicle speed, lining pressure force, braking energy and instantaneous friction coefficient in the linear velocity of the rotating disc.

The waveforms of the instantaneous friction coefficient presented in Figures 7–10 show the behavior of the sintered friction material during the braking simulation at different initial speeds and the assumed parameters of the contact force and the simulated braked masses per brake disc. In the case of Figures 7 and 8, the course of the instantaneous friction coefficient is stable and increasing from the level of approx. 0.290–0.300 (beginning of braking) to the value of the coefficient of approx. 0.350–0.400 at the end of braking. The exception is braking test no. 10, in which the instantaneous coefficient of friction in 110 s of braking gradually decreases to the value of approx. 0.260, creating the so-called saddle". One of the reasons may be the influence of high temperatures above 400 °C on the friction material (long braking time above 110 s) as well as the tribological properties of the friction material itself possibly causing disturbances and instability of the friction coefficient.

During the experimental tests, it was observed that in the initial phase of braking, there is a large amplitude of variability of the instantaneous coefficient of friction, resulting from local instabilities of the contact between the lining and the disc related to appearance of gradients in hot bands.

After analyzing the diagrams above, it can be noticed that the disc temperature rises steadily during the braking and reaches its maximum value at the end. However, a distinctive effect was not recorded. This effect concerns a slight drop in the disc frictional surface temperature at the end of the braking process (with low speed and amount of heat generated). It may arise from imperfect slip thermocouple measurements. In this case, the temperature measurement is disturbed between the thermocouple and the friction surface of the disc brake. The generated heat is taken into account in the measurement of the surface temperature of the disc; therefore, it is advisable to use other tools to verify this method.

In addition, infrared thermography was used in experimental research. Such a non-destructive measuring method allowed characterization of the thermal phenomena in the braking elements of rail vehicles and their impact on changes in the properties of elements. Experimental research is an essential instrument for detecting and understanding the physical effects of the mentioned phenomena. The results obtained from such tests can be used to validate theoretical models, which later allow the relationships of complex interactions and thermal, mechanical and tribological effects in the braking systems under consideration during the braking to be described. In Figures 11–14, selected infrared images concerning two analyzed braking cases are presented. The temperature distribution on the disc friction surface can be seen at the end of the braking.

The double representation of Figures 11–14 is intended to present a more accurate temperature distribution on the tested object. In the case of the photos on the left (a), the software of the thermal imaging camera, due to its limitations, can provide a palette of temperature ranges from the minimum to the maximum value. Figures on the right (b) were made by exporting numerical data to MS Excel, where it is possible to increase the number of temperature ranges and thus their better evaluation.

5. Simulation Investigations

5.1. Research Object

The simulations were performed for the disc brake of a high-speed rail vehicle (Figure 15). The basic parameters of this brake are presented in Table 4.

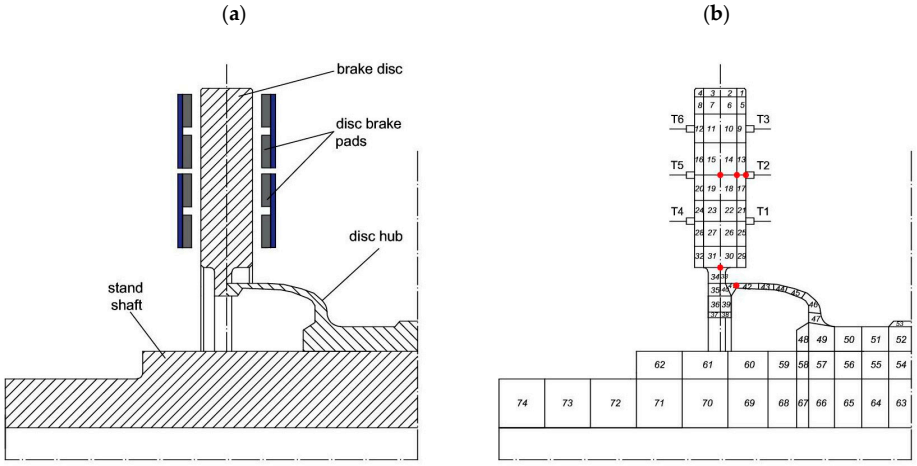

Figure 15. Axial section of a high-speed train brake disc installed on the test stand: (**a**) overview drawing, (**b**) adopted finite element mesh of the brake rotor including additional parts (disc hub, a part of test stand shaft) connected to the brake disc. The location of thermocouples (T_1, T_2, . . . , T_6) is also shown.

Table 4. Technical data of railway brake.

General Parameters of the Brake:		
External diameter of the disc brake (mm)		640
Thickness of the disc brake (mm)		45
Frictional area:	Brake rotor	Friction linings
Disc brake	209,900 (mm^2) 0.2099 (m^2)	40,000 (mm^2) 0.0400 (m^2)
Material parameters:	**Cast steel disc**	**Friction linings**
Heat conduction coefficient (W/mK)	45	2.4
Density (kg/m^3)	7300	5250
Specific heat (J/kgK)	615	1600

The material from which the considered disc brakes are made is cast steel. The relationships for heat conduction coefficient $\lambda(T)$ and specific heat $c_p(T)$ were analyzed for this material. However, it should be noted that the material data were obtained from thermodynamic tables and not directly from the disc brake manufacturer.

It can be concluded that the thermal conductivity coefficient λ decreases mildly with increasing temperature. However, changes in this coefficient in the temperature range of interest to us (50–500 °C) are relatively small. In turn, the specific heat c_p increases with increasing temperature, but the increase is not large.

For the above reasons, the heat transfer problem can be considered linear in the range of moderate temperatures. That is why the averaged material properties for the predicted temperature range were applied.

It should be emphasized that the tests were carried out for one axial disc brake and one set of brake linings (four pads). For this reason, a symmetry plane can be found on the right side of Figure 15a. Normally, there may be two, three or four brake discs on the axle of the train, depending on the required maximum speed of the train and the braking energy.

Figure 15b shows the adopted mesh of the disc's finite elements, including additional parts (such as the disc hub and a part of the test stand shaft) connected to the disc brake. Figure 15b also distinguishes five mesh nodes where the temperature variations over time are given. These points apply to the center of the frictional surface and two different depths under this surface up to the center of the disc thickness, i.e., 8 mm and 22.5 mm. Two other points are placed at the inner part of the disc brake and on the disc hub (see Figure 15b). Figure 15b presents the location of slip thermocouples (T_1, T_2, . . . , T_6) of the brake under consideration. It should be noticed that all the points of the thermocouple location coincide with the location of the corner nodes or nodes in the middle of the edges of finite elements.

5.2. Results of Numerical Calculations

The purpose of numerical simulations was to reconstruct the heat transfer conditions available during previously described (Section 4) experimental tests of the disc brake on the inertial test bench.

The calculations were performed for all four tests (Table 2). The initial temperature differed for each measurement. The same values were assumed in the computer simulations. On the other hand, the ambient temperature was assumed each time as 20 °C, i.e., analogous to that in the experimental investigations.

Figure 16 shows the time courses for forwarding train speed and angular velocity of the disc brake reconstructed on the inertial test bench. In the case of intensive braking until a halt, both values decline almost linearly over braking time. The initial speeds of the rail vehicle are high and equal from 200 to 350 km/h, which applies to angular velocities of the disc brake cca. 130–220 rad/s. The inertial test bench ensured sufficiently high brake thermal loads, similar to those existing when the rail vehicle brakes in actual conditions, and similar sliding speed to that of brake friction pairs [16].

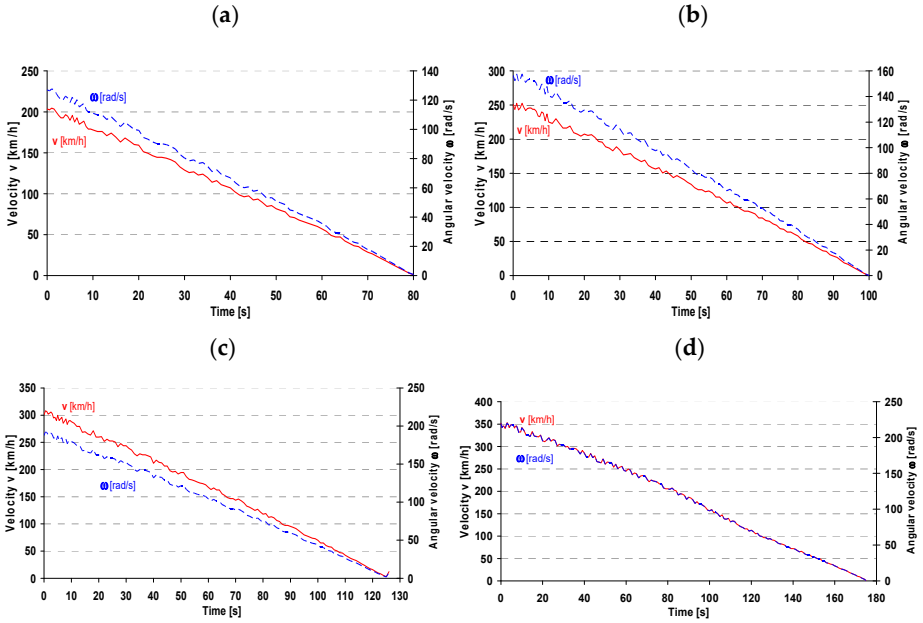

Figure 16. Simulated train forward speed and angular velocity of the disc brake tested on the inertial bench versus time. Braking from the initial speed of (**a**) v_0 = 200 km/h (test no. 2), (**b**) v_0 = 250 km/h (test no. 3), (**c**) v_0 = 300 km/h (test no. 4), (**d**) v_0 = 350 km/h (test no. 10).

The heat transfer rate generated in the brake $Q'(t)$ was established based on available time courses of braking torque $M_H(t)$ and angular velocity $\omega(t)$ of the inertial bench shaft, and therefore for the disc brake under consideration:

$$\dot{Q}(t) = M_H(t) \cdot \omega(t) = F_r(t) \cdot r_r \cdot \frac{\pi \cdot n(t)}{30} \tag{7}$$

where:

$F_r(t)$, $n(t)$—measured time courses of the force on the reaction arm r and the test bench shaft rotational speed.

Next, the time course for the heat flux $q'(t)$ penetrating the disc was calculated. It equals the heat rate $Q'(t)$ divided by the friction surface of the considered disc brake. However, it should be noted that the coefficient ξ (see Equation (3)), i.e., the ratio of heat flux partition between the rotor and friction linings, is also considered. The coefficient ξ depends on the material properties of the friction pair. The time courses of $Q'(t)$ and $q'(t)$ are depicted in Figure 17.

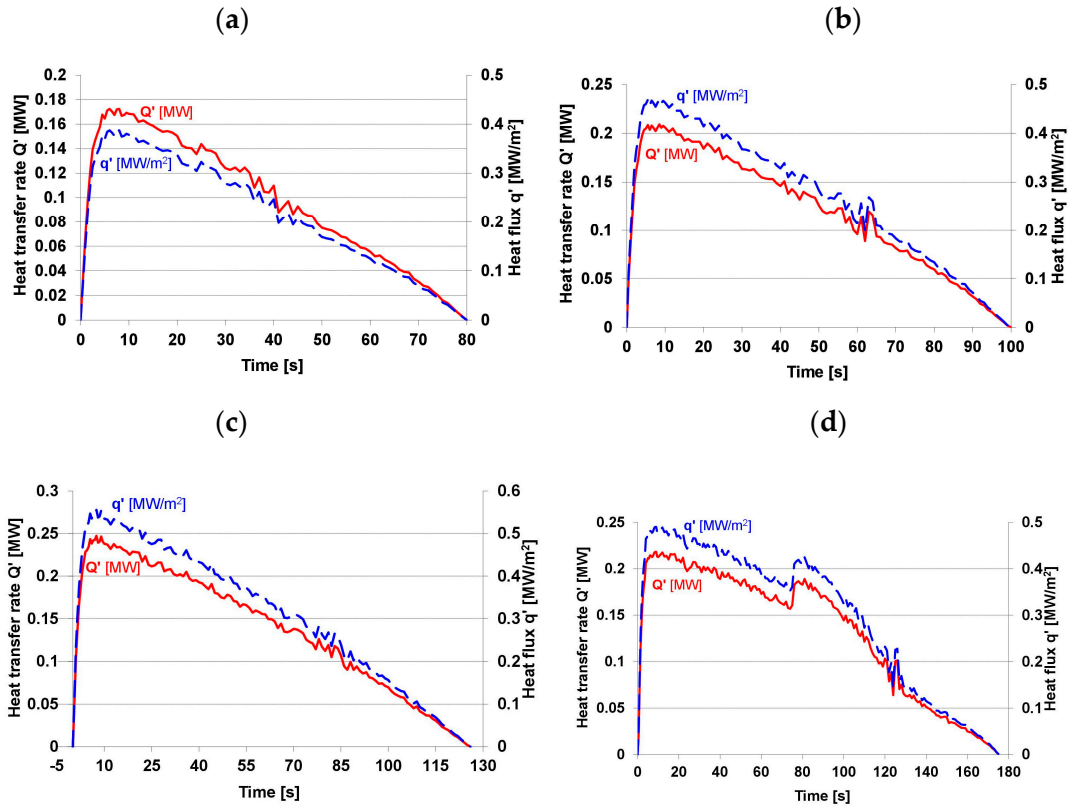

Figure 17. Heat transfer rate Q′ (W) generated in the disc brake and heat flux q′ (W/m^2) on its frictional surface versus time. Braking from the initial speed of (**a**) v_0 = 200 km/h, (**b**) v_0 = 250 km/h, (**c**) v_0 = 300 km/h, (**d**) v_0 = 350 km/h.

At first, after applying the brake, a significant increase in the heat transfer rate generated in the brake can be observed. Then, both $Q'(t)$ and $q'(t)$ drop almost linearly to zero as the braking time passes. The reason for this is the continuous decrease in the sliding speed of the friction pairs during the braking. The heat transfer to the environment occurs on the free surfaces of the railway brake. These are the disc and additional parts, such as the disc hub and a part of the test stand shaft connected to the disc brake (see Figure 18).

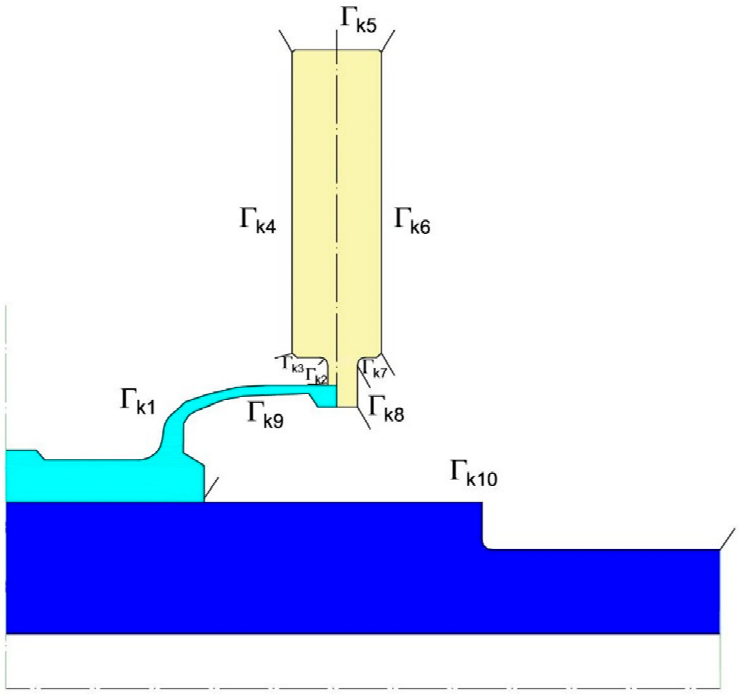

Figure 18. Free surfaces (Γ_{ki}, $i = 1, 2, \ldots, 10$) of heat transfer with the environment concerning the disc brake installed on the test stand.

Table 1 on free surfaces (Γ_{ki}, $i = 1, \ldots, 10$) were applied for this research object. The relations concerning heat transfer coefficients on these surfaces (disc, external and internal cylindrical) were given in References [47–49].

(1) Convective heat transfer coefficient α_k for the disc surface:

$$\alpha_k = \frac{0.076}{(2\pi)^{0.2}} \lambda_{air} r_{av}^{0.6} \left(\frac{\omega}{\nu_{air}} \right)^{0.8} \tag{8}$$

where:

λ_{air}—thermal conductivity of air in the boundary layer;
ν_{air}—kinematic viscosity of air in the boundary layer;
r_{av}—average radius of the disc surface;
ω—angular velocity of the disc.

(2) Convective heat transfer coefficient α_k for the external cylindrical surface:

$$\alpha_k = 0.135 \frac{\lambda_{air}}{D} \left[\left(0.5 Re_r^2 + Re_s^2 + Gr \right) Pr \right]^{\frac{1}{3}} \tag{9}$$

where:

D—cylinder diameter;
Re_r—Reynolds number for the rotational air flow;
Re_s—Reynolds number for the transverse outflow of the cylinder;
Gr—Grashof number;
Pr—Prandlt number.

(3) Convective heat transfer coefficient α_k for the internal cylindrical surface:

$$\alpha_k = 0.14 \lambda_{air} \left[\beta \frac{\omega^2 D (T - T)}{2 \nu_{air}^2} Pr \right]^{\frac{1}{3}} \tag{10}$$

where:

β—volumetric expansion coefficient of air;
ω—angular velocity of the rotating surface;
D—diameter of the internal cylindrical surface;
T—surface temperature;
T_∞—ambient temperature.

Figure 19 shows the time courses for the heat transfer coefficients α_{ki} on the disc brake's free surfaces (Γ_{ki}, $i = 1, \ldots, 10$). The heat transfer coefficient values (Figure 19) decline with a drop in rail vehicle speed and with the brake flow-round intensity. The time courses presented in Figure 19 served as boundary conditions of the III type in the developed heat conduction model (Equations (4),(5)). The free surfaces of the disc brake mounted on the test stand were divided into: (1) disc surface, (2) cylindrical and (3) internal cylindrical. The following coefficients of heat transfer with the environment correspond to these surfaces: (1) α_{k2}, α_{k4}, α_{k6}, α_{k8}, (2) α_{k1}, α_{k5}, α_{k10} and (3) α_{k3}, α_{k7}, α_{k9}. All these heat transfer coefficients are shown in Figure 19.

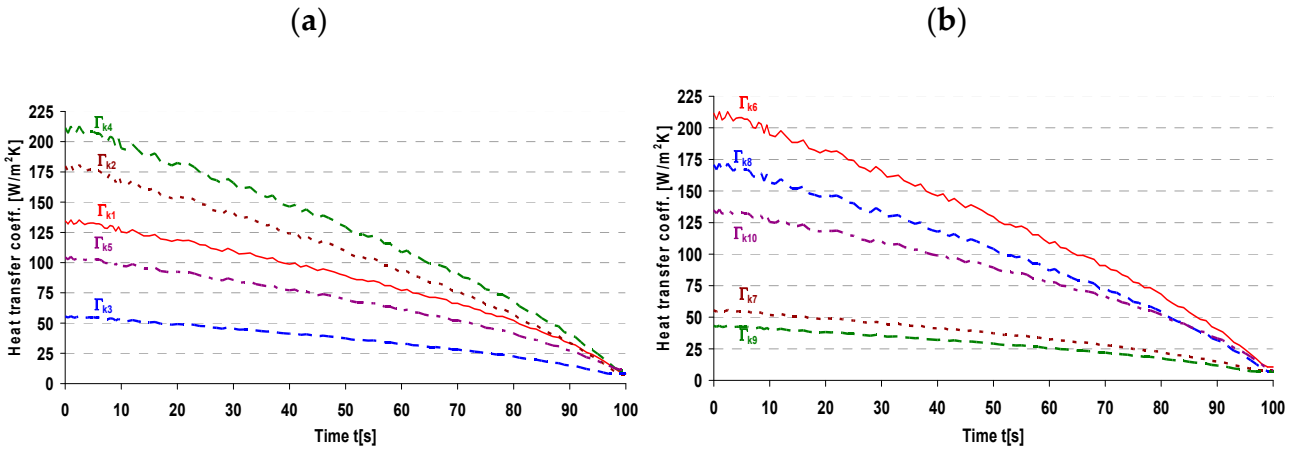

Figure 19. Heat transfer coefficients α_{ki} on free surfaces Γ_{ki} of the disc brake (installed on the test stand) versus time: (**a**) on surfaces (Γ_{ki}, $i = 1, \ldots, 5$), (**b**) on surfaces (Γ_{ki}, $i = 6, \ldots, 10$). Braking from the initial speed of $v_0 = 250$ km/h.

The convective heat transfer between the air and the brake rotor surfaces is the primary means of heat rejection. Radiation heat transfer is less important than convective, especially for low surface temperatures. However, it was also considered in the analysis—the averaged radiation heat transfer coefficients α_{ri} for the predicted temperature range were calculated.

Figure 20 shows the time courses for temperatures at five chosen points of the disc section (Figure 20b), including the friction surface. As expected, the temperature courses at all points are nearly monotonous. The fastest growth in temperature is observed on the disc friction surface, where the heat is generated. The further from this surface, the milder the temperature increase at this point. The calculated temperatures apply to the center of the frictional surface and 8 mm and 22.5 mm under this surface. Two other points are placed at the inner part of the disc brake and on the disc hub (see Figure 20b). When a small amount of heat is generated in the final braking stage, the temperature on the frictional surface drops slightly. The rise of the heat outflow to other parts of the brake rotor can be noticed. Similar temperature courses have been confirmed in many works, including some by one of the authors of this publication [7,13,26].

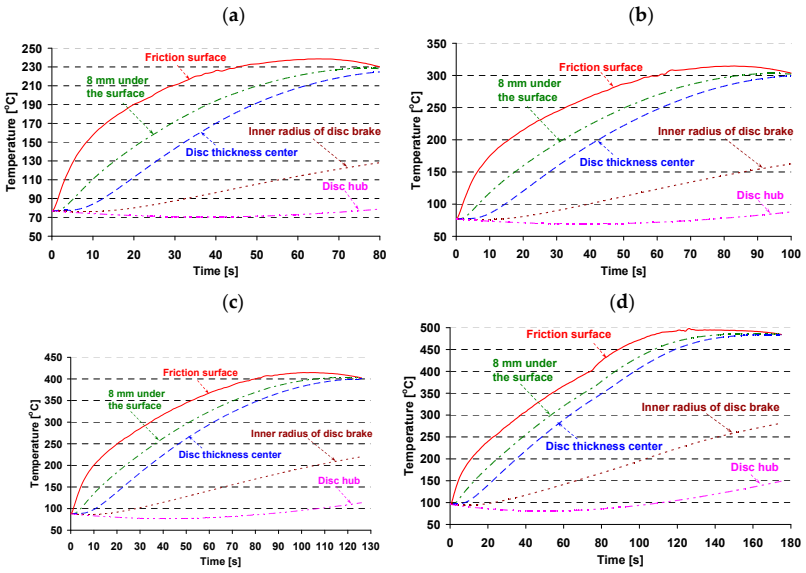

Figure 20. Temperature T_i at five selected points (see Figure 15b) of the disc brake versus time. Calculated temperatures concern friction surface, 8 and 22.5 mm under this surface, at the inner part of the disc brake and hub. Braking from the initial speed of (**a**) v_0 = 200 km/h, (**b**) v_0 = 250 km/h, (**c**) v_0 = 300 km/h, (**d**) v_0 = 350 km/h.

Figure 21 presents isotherms at the axial cross-section of the brake disc at the end of braking time on the test stand. Calculated temperatures concern the end of braking from the initial speed of (a) v_0 = 200 km/h, (b) v_0 = 250 km/h, (c) v_0 = 300 km/h, (d) v_0 = 350 km/h. For each case, the highest temperature reached can be observed near the friction surface of the disc brake. It should be noted that there are high temperature gradients near the rubbing surface. The temperatures of the disc hub are not so high. The lowest temperatures are registered for the test stand shaft.

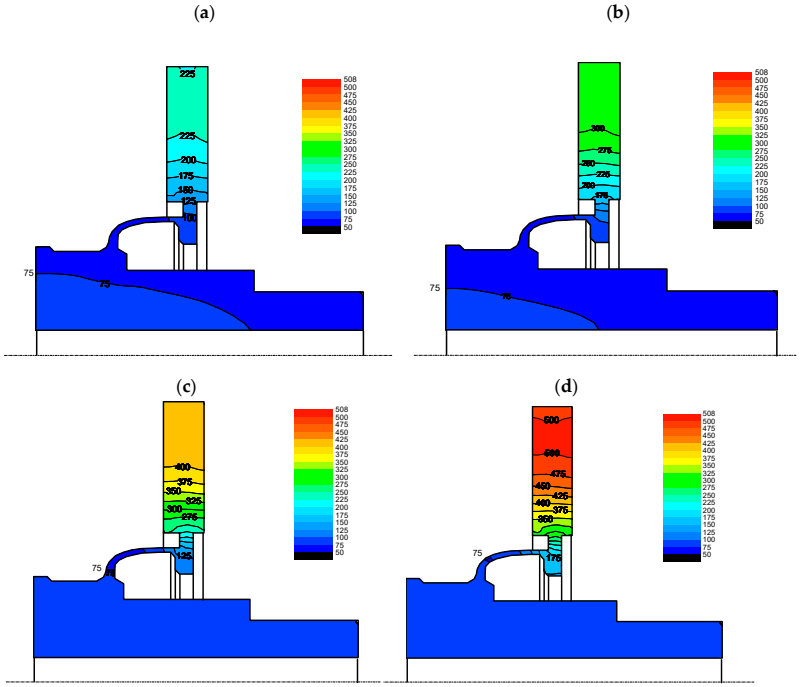

Figure 21. Isotherms (°C) in the cross-section of the disc brake installed on the test stand. Calculated temperatures concern the end of braking t_b (s) from the initial speed of (**a**) v_0 = 200 km/h, t_b = 80 s, (**b**) v_0 = 250 km/h, t_b = 100 s, (**c**) v_0 = 300 km/h, t_b = 126 s, (**d**) v_0 = 350 km/h, t_b = 175 s.

6. Comparison of Simulation and Experimental Test Results

Figure 22 presents the time courses for temperatures on two friction surfaces of the disc, measured by six slip thermocouples (see Figure 15b). The calculated time course for the temperature in the center of the frictional surface, near the thermocouples T2 and T5 (Figure 15b), is illustrated. Simultaneously, the results of experimental tests and simulations were subject to preliminary comparison. Similar values of maximum temperatures at the end of braking were achieved, i.e., approx. 230 °C for test no. 2, 300 °C for test no. 3, approx. 400 °C for test no. 4, and 480 °C for test no. 10. A particular discrepancy of time courses for temperatures can be observed during the process under consideration. It is advisable to develop further studies of this issue.

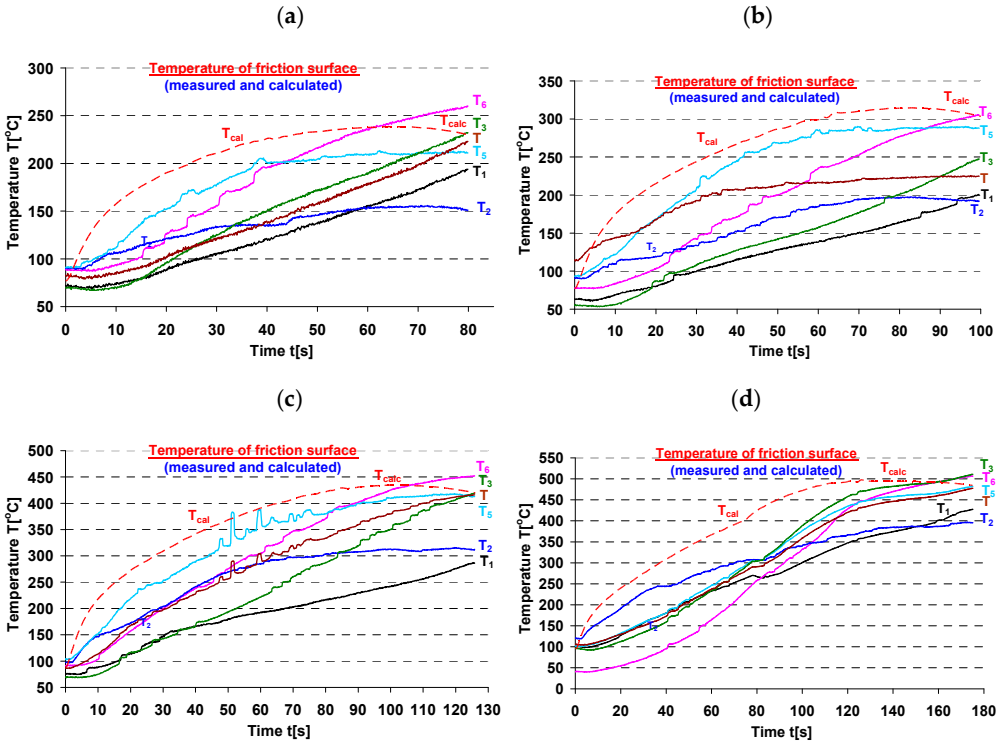

Figure 22. Comparison of measured and calculated temperatures of friction surface of the disc brake during braking. Measured temperatures (T_i, i = 1, . . . , 6) apply to the location of thermocouples (Figure 15b), and the calculated temperature T_{calc} applies to the mesh node on the friction surface (Figure 15b). Braking from the initial speed of (**a**) v_0 = 200 km/h, (**b**) v_0 = 250 km/h, (**c**) v_0 = 300 km/h, (**d**) v_0 = 350 km/h.

Table 5 summarizes the obtained results of temperature measurements (using a thermal imaging camera) and simulation tests.

Table 5. Comparison of the results of infrared measurements and simulation tests.

Test No.	Infrared Camera	Simulation
2—(v_0 = 200 km/h)	208 °C	approx. 230 °C
3—(v_0 = 250 km/h)	264 °C	approx. 300 °C
4—(v_0 = 300 km/h)	378 °C	approx. 400 °C
10—(v_0 = 350 km/h)	480 °C	approx. 480 °C

Differences between the experimental tests using infrared cameras and simulation calculations do not exceed 13%. Differences may result from the adopted emissivity index of the disc brake material during experimental tests.

7. Conclusions

As an essential part of the research, several measurements during braking on the test stand were performed. The most representative and interesting results were chosen for the article. The main criteria of this selection were the high initial speeds (250–350 km/h) and consequently thermal loads of friction pairs.

The experimental tests and simulations should induce further research and aim to use the authors' application in testing the railway brakes. The tests will be continued to check other variants and assumptions related to friction pairs.

Based on the comparison of bench tests and simulations, similar values of maximum temperatures at the end of braking were obtained, i.e., approx. 230 °C for test no. 2, 300 °C for test no. 3, approx. 400 °C for test no. 4 and 480 °C for test no. 10, respectively. However, a particular discrepancy in the time courses of temperatures was recorded during the process under consideration.

Unfortunately, the material properties for both the disc brake and brake pads were taken from the literature because obtaining such information from the manufacturers of friction pairs was impossible.

The measurement was performed correctly. As a result of friction between the sliding thermocouple and the surface of the disc, additional heat is generated, disturbing the measurement itself. For the disc brakes without ventilation channels, it was impossible to embed thermocouples under the friction surface at a depth of 1 mm according to EN 14535 standards. That is why sliding thermocouples were applied in this case. The infrared camera measurements supplement the measurements with the use of sliding thermocouples, the results of which are presented in Figures 11–14 and then discussed and compared with the results of simulation tests.

The results of infrared measurements and numerical simulations (see Figures 11–15) have proved that during a single, relatively short-lasting (ca. 80–175 s) railway braking, the additional brake parts (disc hub, a part of test stand shaft) connected to the brake disc heat up to a negligible degree (approx. 50 °C of temperature increase). Therefore, the thermal capacity of these additional brake parts can be neglected in the case of numerical calculations.

The tests on the inertial bench and simulation program can be used to analyze the heat transfer process in railway brakes, assess or forecast braking effectiveness changes due to the thermal state of brakes and optimize the brake design.

Author Contributions: J.K. and A.W. got the idea for this work. J.K. and S.W. conducted all the measurements on a dynamometric stand for railway brakes. A.W. developed a specialized computer program of the finite element method and conducted all the numerical calculations. J.K. and A.W. prepared the first version of the manuscript, responses to the reviewers and created the final manuscript. All authors have read and agreed to the published version of the manuscript.

Funding: This paper was co-financed under the research grant of the Warsaw University of Technology supporting the scientific activity in the discipline of Civil Engineering, Geodesy and Transport.

Data Availability Statement: The data used to support the findings of this study are available from the corresponding author upon request.

Conflicts of Interest: The authors declare no conflict of interest.

References

1. Anderson, A.E.; Knapp, R.A. Hot spotting in automotive friction systems. *Wear* **1990**, *135*, 319–337. [CrossRef]
2. Konowrocki, R.; Kukulski, J.; Walczak, S.; Groll, W. Distribution of thermal energy in the elements of the braking system of high-speed vehicles. *Pojazdy Szyn.* **2014**, *2*, 1–14. (In Polish)
3. Schuetz, T. *Cooling Analysis of a Passenger Car Disk Brake*; SAE: Warrendale, PA, USA, 2009; Paper 2009-01-3049. [CrossRef]
4. Zienkiewicz, O.C.; Morgan, K. *Finite Elements and Approximation*; John Wiley & Sons, Inc.: Hoboken, NJ, USA, 1983; 328p.
5. Zagrodzki, P. Clutches, Hot Spotting Behavior. In *Encyclopedia of Thermal Stresses*; Hetnarski, R.B., Ed.; Springer: Berlin/Heidelberg, Germany, 2014; pp. 606–614. [CrossRef]
6. Zagrodzki, P.; Truncone, S.A. Generation of hot spots in a wet multidisk clutch during short-term engagement. *Wear* **2003**, *254*, 474–491. [CrossRef]

7. Lozia, Z.; Wolff, A. *Thermal State of Automotive Brakes after Braking on the Road and on the Roll-Stand*; No 1229/SAE Technical Paper No 971040; SAE Special Publication: Warrendale, PA, USA, 1997; pp. 107–115.
8. Hwang, P.; Wu, X.; Jeon, Y.B. Thermal–mechanical coupled simulation of a solid brake disc in repeated braking cycles. *Proc. Inst. Mech. Eng.* **2009**, *223*, 1041–1048. [CrossRef]
9. Jung, S.P.; Park, T.W.; Chai, J.B.; Chung, W.S. Thermo-mechanical finite element analysis of hot judder phenomena of a ventilated disc brake system. *Int. J. Precis. Eng. Manuf.* **2011**, *12*, 821–828. [CrossRef]
10. Kim, J.G.; Kwon, S.T.; Yoon, S.C. Analysis of Hot Spots Evolution on Brake Disc Using High-Speed Infrared Camera. *Key Eng. Mater.* **2010**, *15*, 317–320. [CrossRef]
11. Konowrocki, R.; Groll, W.; Kukulski, J.; Walczak, S. Temperature field analysis of brake discs for high-speed train using infrared technology. In Proceedings of the Advanced Rail Technologies—5th International Conference, Warsaw, Poland, 16 November 2017.
12. Mackin, T.J.; Noe, S.C.; Ball, K.J.; Bedell, B.C.; Bim-Merle, D.P.; Bingaman, M.C.; Bomleny, D.M.; Chemlir, G.J.; Clayton, D.B.; Evans, H.A.; et al. Thermal cracking in disc brakes. *Eng. Fail. Anal.* **2002**, *9*, 63–76. [CrossRef]
13. Nisonger, R.; Yen, C.; Antanaitis, D. High Temperature Brake Cooling—Characterization for Brake System Modeling in Race Track and High Energy Driving Conditions. *SAE Int. J. Passeng. Cars Mech. Syst.* **2011**, *4*, 384–398. [CrossRef]
14. Nouby, M.; Abdo, J.; Mathivanan, D.; Srinivasan, K. Evaluation of Disc Brake Materials for Squeal Reduction. *Tribol. Trans.* **2011**, *54*, 644–656. [CrossRef]
15. Ripley Maurice, I.; Kirstein, O. Residual stresses in a cast iron automotive brake disc rotor. *Phys. B Condens. Matter* **2006**, *385–386*, 604–606. [CrossRef]
16. Wolff, A.; Kukulski, J. Numerical and Experimental Analysis of the Heat Transfer Process in a Railway Disc Brake. *Railw. Rep. Probl. Kolejnictwa* **2019**, *185*, 59–69. [CrossRef]
17. Wolff, A. A method to achieve comparable thermal states of car brakes during braking on the road and on a high-speed roll-stand. *Arch. Transp.* **2010**, *XXII*, 259–273. [CrossRef]
18. Wolff, A. Numerical analysis of heat transfer in cylinder of a marine two-stroke engine. *Combust. Engines* **2015**, *162*, 849–857.
19. Wolff, A. Possibilities to achieve assumed thermal states of automotive brakes during testing on a high-speed roll-stand. *Logistyka* **2010**, *4*, 1–8.
20. Shahzamanian, M.M.; Sahari, B.B.; Bayat, M.; Ismarrubie, Z.N.; Mustapha, F. Transient and thermal contact analysis for the elastic behavior of functionally graded brake disks due to mechanical and thermal loads. *Mater. Des.* **2010**, *31*, 4655–4665. [CrossRef]
21. Wang, L.; Xin, L.; Haoseng, L.; Gong, W.; Wang, L. A new experimental method to study the convective heat transfer characteristics of the interior passages of ventilated disc brakes. *Int. J. Therm. Sci.* **2022**, *179*, 107675. [CrossRef]
22. Cati, Y.; Wiesche, S.; Düzgün, M. Numerical Model of the Railway Brake Disk for the Temperature and Axial Thermal Stress Analyses. *J. Therm. Sci. Eng. Appl.* **2022**, *14*, 101014. [CrossRef]
23. *EN 14535-3:2015*; Railway Applications—Brake Discs for Railway Rolling Stock—Part 3: Brake Discs, Performance of the Disc and the Friction Couple, Classification. International Electrotechnical Commission (IEC): Geneva, Switzerland, 2015.
24. Maniana, M.; Azime, A.; Errchiqui, F.; Tajmouati, A. Analytical and Numerical Analysis of Thermal Transfer in Disc Brake. *Heat Technol.* **2022**, *40*, 693–698. [CrossRef]
25. Wang, L.-L.; Wang, L.; Gao, Z.-X.; Wang, L.-B.; Wang, Y. The convective heat transfer characteristics of the track surface on which wheels roll over periodically. *Int. J. Therm. Sci.* **2021**, *165*, 106947. [CrossRef]
26. Kukulski, J. *Experimental and Simulation Study of Railway Vehicle and the Infrastructure Its Components Safety and Operation Aspect, Wydawnictwo Politechniki Warszawskiej*; Publishing House of the Warsaw University of Technology: Warsaw, Poland, 2016; pp. 1–139. Available online: http://www.wydawnictwopw.pl/index.php?s=karta&id=3260 (accessed on 1 April 2023). (In Polish)
27. Kim, D.-J.; Lee, Y.-M.; Park, J.-S.; Chang-Sung, S. Thermal stress analysis for a disk brake of railway vehicles with considering the pressure distribution on a frictional surface. *Mater. Sci. Eng.* **2008**, *483–484*, 456–459. [CrossRef]
28. Tang, B.; Mo, J.-L.; Wu, Y.K.; Quan, X.; Zhu, M.H.; Zhou, Z.R. Effect of the Friction Block Shape of Railway Brakes on the Vibration and Noise under Dry and Wet Condition. *Tribol. Trans.* **2019**, *62*, 262–273. [CrossRef]
29. Djafri, M.; Bouchetara, M.; Busch, C.; Khatir, S.; Khatir, T.; Weber, S.; Shbaita, K.; Abdel Wahab, M. Influence of Thermal Fatigue on the Wear Behavior of Brake Discs Sliding against Organic and Semimetallic Friction Materials. *Tribol. Trans.* **2018**, *61*, 860–867. [CrossRef]
30. Yevtushenko, A.A.; Kuciej, M.; Grzes, P.; Wasilewski, P. Comparative Analysis of Temperature Fields in Railway Solid and Ventilated Brake. *Materials* **2021**, *14*, 7804. [CrossRef] [PubMed]
31. Grzes, P. Finite element solution of the three-dimensional system of equations of heat dynamics of friction and wear during single braking. *Adv. Mech. Eng.* **2018**, *10*, 1–15. [CrossRef]
32. Yevtushenko, A.A.; Kuciej, M.; Grzes, P.; Wasilewski, P. Temperature in the railway disc brake at a repetitive short-term mode of braking. *Int. Commun. Heat Mass Transfer.* **2017**, *84*, 102–109. [CrossRef]
33. Zewang, Y.; Chun, T.; Mengling, W.; Guozhuang, W. A modified uniformly distributed heat source method for predicting braking temperature of railway brake disc. *Int. J. Rail Transp.* **2021**, *10*, 216–229. [CrossRef]
34. Sha, Z.; Lu, J.; Hao, Q.; Yin, J.; Liu, Y.; Zhang, S. Numerical Simulation of Heat Production and Dissipation of Ventilated Brake Disc for High-Speed Trains under the Action of the Flow Field. *Appl. Sci.* **2022**, *12*, 10739. [CrossRef]
35. Barber, J.R. Thermoelastic instabilities in the sliding of conforming solids. *Proc. R. Soc. Lond.* **1969**, *312*, 381–394. [CrossRef]

36. Eriksson, M.; Filip Bergman, F.; Jacobson, S. On the nature of tribological contact in automotive brakes. *Wear* **2002**, *252*, 26–36. [CrossRef]
37. Kao, T.; Richmond, J.W.; Douarre, A. Brake disc hot spotting and thermal judder: An experimental and finite element study. *Int. J. Vehicle Des.* **2011**, *23*, 276–296. [CrossRef]
38. Kim, M. Development of the Braking Performance Evaluation Technology for High-speed Brake Dynamometer. *Int. J. Syst. Appl. Eng. Dev.* **2012**, *6*, 2012.
39. Eriksson, M.; Jacobson, S. Tribological surfaces of organic brake pads. *Tribol. Int.* **2000**, *33*, 817–827. [CrossRef]
40. Jung, S.P.; Park, T.W.; Lee, J.H.; Kim, W.H.; Chung, W.S. Finite element analysis of thermoelastic instability of disc brakes. In Proceedings of the World Congress on Engineering, London, UK, 30 June–2 July 2010.
41. Fischer, S.; Sardá, A.; Winner, H. Effects of Different Friction Materials on Hot Judder—An Experimental Investigation. In Proceedings of the EuroBrake 2013 Conference, Dresden, Germany, 17–19 June 2013; EB2013-TE-005.
42. Palmer, E.; Mishra, R.; Fieldhouse, J.; Layfield, J. *Analysis of Air Flow and Heat Dissipation from a High-Performance GT Car Front Brake*; SAE Paper: Warrendale, PA, USA, 2008; Volume 2008-01-0820. [CrossRef]
43. Graf, M.; Ostermeyer, G.-P. Hot bands and hot spots: Some direct solutions of continuous thermoelastic systems with friction. *Phys. Mesomech.* **2012**, *15*, 306–315. [CrossRef]
44. Yildiz, Y.; Duzgun, M. Stress analysis of ventilated brake discs using the finite element method. *Int. J. Automot. Technol.* **2010**, *11*, 133–138. [CrossRef]
45. Wang, D.; Wang, R.; Heng, T.; Xie, G.; Zhang, D. Tribo-Brake Characteristics between Brake Disc and Brake Shoe during Emergency Braking of Deep Coal Mine Hoist with the High Speed and Heavy Load. *Energies* **2020**, *13*, 5094. [CrossRef]
46. Incropera, F.P.; DeWitt, D.P.; Bergman, T.L.; Lavine, A.S. *Fundamentals of Heat and Mass Transfer*; John Wiley & Sons: Hoboken, NJ, USA, 2006.
47. Hartter, L.; Schwartz, H.; Rhee, S. *Evaluating Copper Alloy Brake Discs by Thermal Modeling*; SAE Transactions: Warrendale, PA, USA, 1974; p. 740560.
48. Kays, W.; Bjorklund, I. *Heat Transfer from a Rotating Cylinder with and without Crossflow*; No 1; ASME Transactions: Little Falls, NJ, USA, 1958.
49. Saumweber, E. *Temperaturberechnung in Bremsscheiben Fuer ein Beliebiges Fahrprogramm*, Leichtbau der Verkehrsfahrzeuge 13, Nr 3; Augsburg, Germany, 1969.